

# PHYSICAL REVIEW B

## CONDENSED MATTER

THIRD SERIES, VOLUME 43, NUMBER 1 PART B

1 JANUARY 1991

### Cation distribution and magnetic properties of titanomagnetites $\text{Fe}_{3-x}\text{Ti}_x\text{O}_4$ ( $0 \leq x < 1$ )

Z. Kąkol, J. Sabol,\* and J. M. Honig

*Department of Chemistry, Purdue University, West Lafayette, Indiana 47907*

(Received 5 June 1990)

Magnetization measurements are presented for the  $\text{Fe}_{3-x}\text{Ti}_x\text{O}_4$  series in the range  $0 \leq x < 1$ . A new model of  $\text{Fe}^{3+}$ - $\text{Fe}^{2+}$  cation distribution is proposed based on saturation-magnetization data. A tilting of the easy magnetization axis away from the [001] direction was encountered at temperatures approaching 4.2 K for the titanium-rich specimens. Anomalies in the hysteresis parameter in the temperature range 40–100 K are reported. A distribution of  $\text{Fe}^{2+}$ ,  $\text{Fe}^{3+}$ , and  $\text{Ti}^{4+}$  ions on tetrahedral and octahedral sites is proposed on the basis of saturation magnetization measurements, which differs to some extent from earlier models published in the literature.

#### INTRODUCTION

Titanomagnetites of composition  $\text{Fe}_{3-x}\text{Ti}_x\text{O}_4$  have been the subject of numerous investigations which document their complex magnetic behavior, particularly at low temperatures and at high Ti concentrations.

The magnetocrystalline anisotropy of titanomagnetites was found by Syono and Ishikawa<sup>1,2</sup> to rise very steeply below 200 K with increasing  $x$ . The various parameters characterizing hysteresis loops were studied in polycrystalline materials by Banerjee *et al.*<sup>3</sup> at 77 K and by Schmidbauer and Readman<sup>4</sup> in the temperature range 4.2–300 K. Both the remanence and the coercive force increased rapidly at low temperatures in the composition range  $x \geq 0.5$ .  $\text{Fe}_{3-x}\text{Ti}_x\text{O}_4$  with  $x > 0$  crystallizes as a mixed inverse spinel:  $\text{Ti}^{4+}$  occupies only the octahedral sites whereas  $\text{Fe}^{2+}$  and  $\text{Fe}^{3+}$  occupy both the octahedral and tetrahedral sites; the concentration of  $\text{Fe}^{2+}$  and  $\text{Fe}^{3+}$  varies with  $x$ . At low temperatures titanomagnetites with  $x \rightarrow 1$  exhibit a tetragonal distortion<sup>5</sup> associated with deviations of the spontaneous magnetization by about  $10^\circ$ – $20^\circ$  from the  $\langle 100 \rangle$  direction.<sup>6</sup> The direction of tetragonal elongation can be changed by the application of a magnetic field.<sup>7,8</sup>

The above magnetic and crystallographic properties were interpreted<sup>6,9</sup> in terms of the large magnetostriction effects reported by several authors.<sup>1,2,7</sup> This magnetostriction was linked<sup>10</sup> to the  $l$ - $s$  coupling of the  $\text{Fe}^{2+}$  ions on octahedral sites and to the Jahn-Teller distortion attributed to  $\text{Fe}^{2+}$  ions on tetrahedral sites.

The presence of  $\text{Fe}^{2+}$  on tetrahedral sites also affects all other magnetic properties of the titanomagnetite system. It is therefore important to know how the occupancy of the octahedral and tetrahedral sites by  $\text{Fe}^{2+}$  and by  $\text{Fe}^{3+}$  varies with  $x$  in  $\text{Fe}_{3-x}\text{Ti}_x\text{O}_4$ . As detailed below, there is considerable disagreement among the findings re-

ported by various investigators.<sup>11–14</sup> These discrepancies have been linked<sup>15–17</sup> to the temperature dependence of the cation distribution as preserved in the quenching process. On the other hand, no changes in physical properties with alterations in thermal history have been detected by other authors.<sup>18,19</sup> In our own work we have introduced a quenching methodology that was found to yield reproducible results; we therefore attempted to determine accurately the cation distribution in the  $\text{Fe}_{3-x}\text{Ti}_x\text{O}_4$  series. This information is needed particularly to analyze the compositional dependence of magnetic properties.

Only a limited number of measurements of saturation magnetization have been reported by the above-mentioned authors on single crystal specimens at or below liquid nitrogen temperatures. The use of ceramic specimens presents difficulties in the interpretation of data, due to the random distribution of crystallographic axes, and because it is difficult to achieve a uniform distribution of  $\text{Ti}^{4+}$  in the samples. In particular,  $\text{Ti}^{4+}$  tends to aggregate at grain boundaries in such specimens.

In this paper, systematic studies of magnetic properties of  $\text{Fe}_{3-x}\text{Ti}_x\text{O}_4$  single crystals with  $0 \leq x < 1$  are reported for the temperature range 4.2–300 K.

#### EXPERIMENT

Single crystals were grown in a CO-CO<sub>2</sub> atmosphere in a skull melter by techniques detailed elsewhere.<sup>20</sup> Using this procedure it was possible to maintain a given charge above its melting point for several hours. Convective stirring optimized the uniform distribution of  $\text{Ti}^{4+}$  in the host material. The titanium distribution and actual composition were checked for each crystal before annealing, using a microprobe electron analyzer, and by energy dispersive analysis of x rays. In the center of the frozen boule from which crystals were removed the actual composition was close to the nominal one. Single crystals,

approximately  $4 \times 4 \times 8 \text{ mm}^3$ , were then reannealed under the appropriate CO-CO<sub>2</sub> gas mixture<sup>21</sup> using an oxygen transfer cell<sup>22</sup> to monitor the oxygen fugacity. Annealing conditions were selected so as to attain the ideal, stoichiometric 4:3 oxygen-to-cation ratio for each specimen.<sup>23,24</sup> The uncertainty in the oxygen stoichiometry was estimated to be  $4 \pm 0.0001$ . Anneals were carried out in the temperature range 1200°–1400 °C (depending on Ti<sup>4+</sup> concentration) for 48 h; the material was then rapidly quenched and trimmed to obtain specimens of uniform oxygen and titanium composition. Each sample was subsequently ground into a small sphere of 1.5–2-mm diameter. Since the sample volume was only a very small fraction (2 to 4%) of the original crystal, each sphere was cut open after completion of the measurements and the Ti composition was checked using the microprobe analyzer. Within the instrumental resolution the samples were found to be homogeneous. The accuracy of the  $x$  determination was therefore limited by the quality of the standard (ilmenite, FeTiO<sub>3</sub>) used in analysis. The error in  $x$

was estimated to be smaller than  $\Delta x = \pm 0.001$ .

Magnetization measurements were carried out with a vibrating sample magnetometer in the temperature range 4.2–300 K and in magnetic fields up to 15 kOe. Magnetization curves and hysteresis loops were measured along the principal crystal directions. Here and below we present only a limited portion of the magnetic measurements which is representative of a much larger data collection. Additional curves will be presented in future publications; the complete set is also available upon request from the authors.

## RESULTS

Representative magnetization curves at room temperature are shown in Fig. 1(a) for a sample with  $x=0.36$ . The temperature variation of the magnetization along the  $\langle 110 \rangle$  direction for a sample with  $x=0.55$ , is presented in Fig. 1(b), as representative of Ti-rich samples; one should note the axis switching at low temperatures.

Samples with  $x > 0.5$  exhibit marked hysteresis effects at low temperatures. It was therefore necessary to measure magnetic moment  $M(H)$  curves on demagnetized samples. Accordingly, samples were warmed above their Néel temperatures  $T_N < 300 \text{ K}$ , cooled in zero field, and

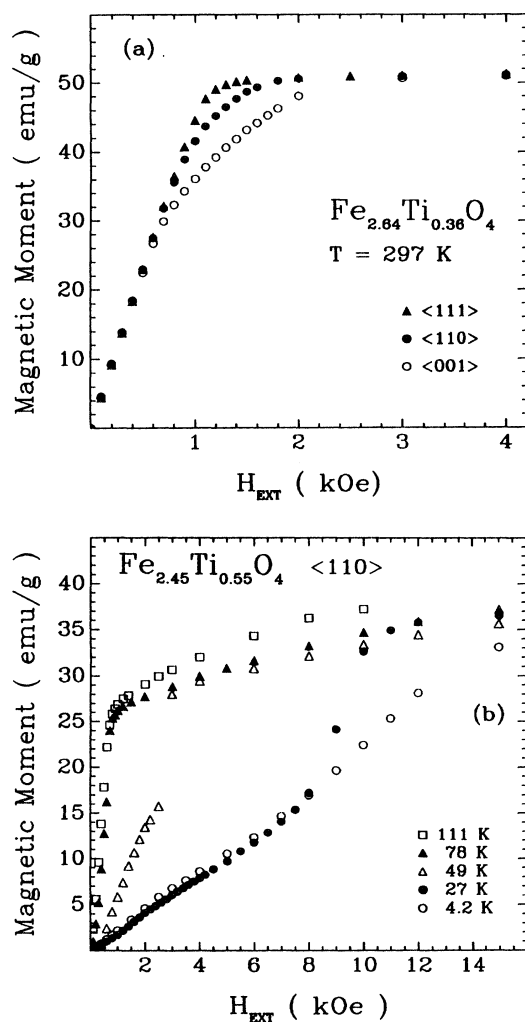


FIG. 1. (a) Magnetization curves of  $\text{Fe}_{2.64}\text{Ti}_{0.36}\text{O}_4$  for  $\langle 111 \rangle$ ,  $\langle 110 \rangle$ , and  $\langle 001 \rangle$  axes at room temperature. (b) Magnetization curves of  $\text{Fe}_{2.45}\text{Ti}_{0.55}\text{O}_4$  along the  $\langle 110 \rangle$  direction in the temperature range 4.2–111 K.

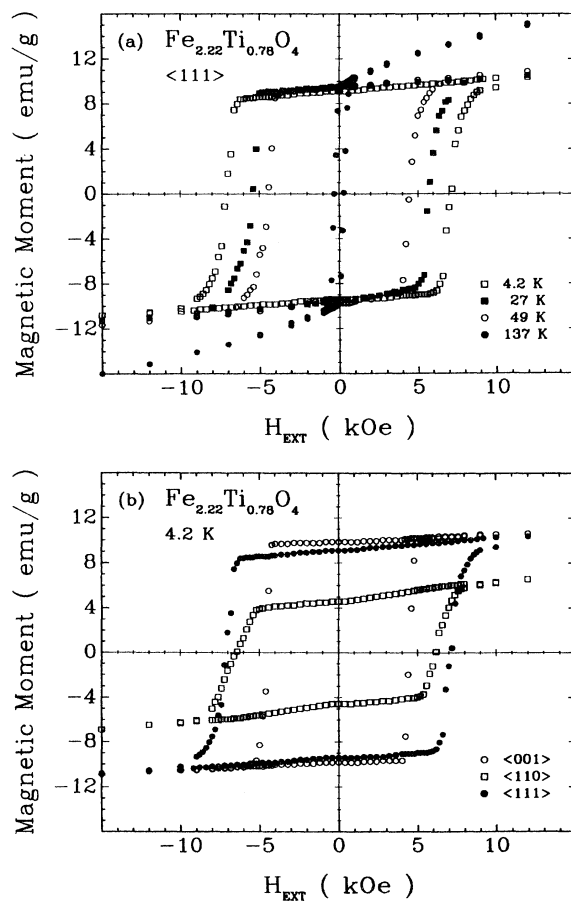


FIG. 2. (a) Hysteresis loops of  $\text{Fe}_{2.22}\text{Ti}_{0.78}\text{O}_4$  along the  $\langle 111 \rangle$  direction in the temperature range 4.2–137 K. (b) Hysteresis loops of  $\text{Fe}_{2.22}\text{Ti}_{0.78}\text{O}_4$  along the  $\langle 111 \rangle$ ,  $\langle 110 \rangle$ , and  $\langle 001 \rangle$  axes at 4.2 K.

data were then collected with the applied field oriented along selected directions. This procedure was repeated for each composition. Our measurements of the variation of the  $T_N$  with  $x$  coincides with data reported in the literature.<sup>25</sup>

Figures 2(a) and 2(b) show representative hysteresis loops for the sample with  $x \approx 0.78$  at selected temperatures and for different crystal orientations. Since the magnetization curves and hysteresis loops along various directions are quite different we determined the angular dependence of magnetization  $M(\theta)$  at fixed fields. A magnetic field was applied along a given direction  $\theta$  and the magnetization was determined; the magnetic field was then switched off and the remanence was measured. The sample was subsequently rotated by 10 degrees and the procedure was repeated.

A remarkable  $M(\theta)$  dependence, explained below, was found for samples with  $x=0.78$  and  $x=0.96$ . The angular dependence of magnetization in the  $(1\bar{1}0)$  and  $(010)$  planes at 4.2 K for the specimen with  $x=0.78$  is shown in

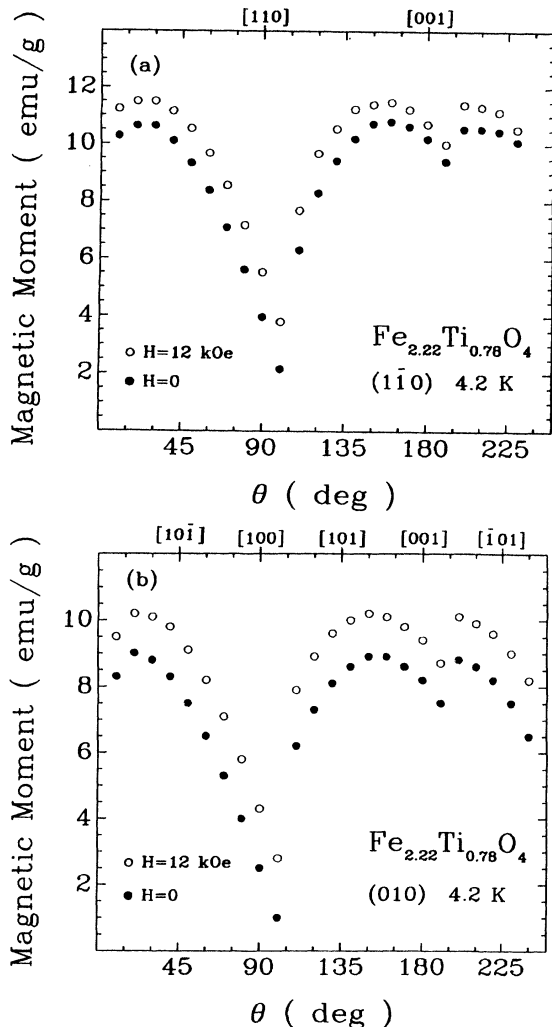


FIG. 3. (a) Angular dependence of the magnetization of  $\text{Fe}_{2.22}\text{Ti}_{0.78}\text{O}_4$  in the  $(1\bar{1}0)$  plane at 4.2 K. (b) Angular dependence of the magnetization of  $\text{Fe}_{2.22}\text{Ti}_{0.78}\text{O}_4$  in the  $(010)$  plane at 4.2 K.

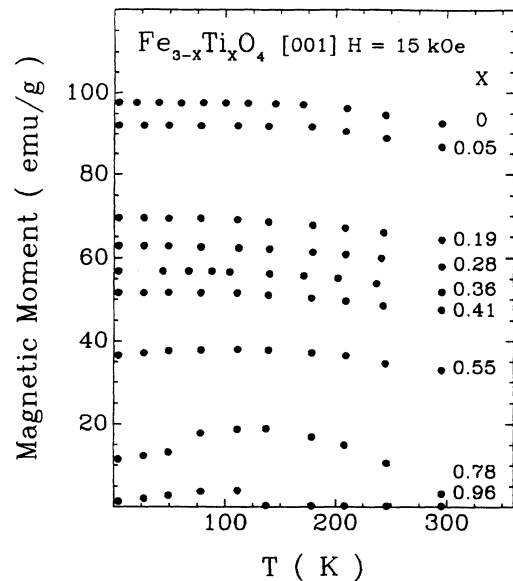


FIG. 4. Temperature dependence of the magnetization of  $\text{Fe}_{3-x}\text{Ti}_x\text{O}_4$  series, along the  $\langle 001 \rangle$  direction in a field  $H=15$  kOe.

Figs. 3(a) and 3(b), respectively.

Finally, the temperature dependence of the magnetization in a magnetic field of 15 kOe was measured along main cubic axes. Results along the  $[001]$  direction are presented in Fig. 4.

#### ANALYSIS OF THE RESULTS

According to Blasse<sup>26</sup> and Wechsler *et al.*<sup>18</sup> titanium enters magnetite exclusively as  $\text{Ti}^{4+}$  into the octahedral sublattice. However, as mentioned earlier, the distribution of  $\text{Fe}^{2+}$  and  $\text{Fe}^{3+}$  among the tetrahedral and octahedral sites is still uncertain. Three different models have so far been advanced; these are shown schematically in Fig. 5. The first is due to Akimoto *et al.*<sup>11</sup> who proposed

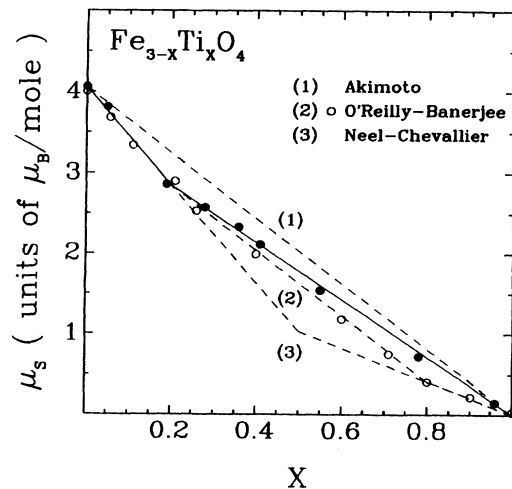


FIG. 5. Variation of saturation magnetization with composition parameter  $x$  for various models of cationic distributions cited in the literature; see text. Open circles, data of Ref. 14; solid circles, present data. Dotted lines represent model calculations of Refs. 11–14; solid line, calculations based on present model.

that the concentration of  $\text{Fe}^{2+}$  and  $\text{Fe}^{3+}$  ions on both sites varies linearly with  $x$ . The second model is due to Néel<sup>12</sup> and Chevallier *et al.*;<sup>13</sup> here, for  $x \leq 0.5$ , the tetrahedral sites are occupied exclusively by  $\text{Fe}^{3+}$  ions, as postulated by Verwey and Heilmann,<sup>27</sup> whereas  $\text{Fe}^{2+}$  also appears randomly on tetrahedral sites when  $x > 0.5$ , i.e., when  $\text{Fe}^{3+}$  can no longer be accommodated on octahedral interstices. The third model, proposed by O'Reilly and Banerjee,<sup>14</sup> is based on their saturation magnetization measurements at 77 K. For  $\text{Ti}^{4+}$  compositions up to  $x \approx 0.2$  this model coincides with the Néel-Chevallier model. In the range  $0.2 < x < 0.8$  additional  $\text{Fe}^{2+}$  ions enter on tetrahedral sites so that both interstitial sublattices now contain ions of both valencies. For  $x \geq 0.8$  it is no longer possible to maintain  $\text{Fe}^{3+}$  on octahedral sites and the model then merges with that of Néel and Chevallier.

Our measurements of the saturation moments at 77 K vs  $\text{Ti}^{4+}$  composition are shown in Fig. 5; with the available field up to 15 kOe samples with  $x > 0.5$  could not be saturated at 4.2 K. For specimens with  $x < 0.5$  the saturation moments at 77 K did not differ significantly from those taken at 4.2 K. The saturation problems stem from the fact that the tetragonal distortion in titanomagnetites rapidly increases with  $x$  for  $x \geq 0.55$ .<sup>5</sup> Our data at 77 K coincide with the Néel-Chevallier and O'Reilly-Banerjee models up to  $x = 0.2$ . However, for larger  $x$  our data lie somewhat higher than those reported by O'Reilly and Banerjee.<sup>14</sup> Their saturation moments on titanium-rich compositions may be low because they used polycrystalline samples: due to the random orientation of crystallites, the applied field coincided with the easy magnetization axis in only a portion of their specimens. Saturation along the hard or intermediate axes is very difficult to achieve for samples with high  $x$  at low temperatures. Even our own results along the [001] direction may represent an underestimate of the saturation in specimens with  $x = 0.78$  and  $x = 0.96$  because this direction is now no longer an easy axis of magnetization: in determining the angular dependence of magnetization up to  $x = 0.55$  the axis of each magnetization remains aligned with one of the principal cubic directions. However, characteristic cusps in the  $M(\theta)$  curves near the [001] direction for the sample with  $x = 0.78$  [see Figs. 3(a) and 3(b)] suggest that the easy axis is now tilted away from the [001] direction by 15 to 25° at 4.2 K. The same deviation was encountered for the sample with  $x = 0.96$ , which is consistent with the observation that the tetragonal distortions for  $x = 0.78$  and  $x = 0.96$  do not differ significantly.<sup>5</sup> Unfortunately, the plane of the deviation was not determined.

The above deviations are in good agreement with data by Kose *et al.*<sup>6</sup> They reported for  $\text{Fe}_2\text{TiO}_4$  at 77 K a deviation of the easy axis by 10–20° away from the [001] direction for both squeezed and stress-free specimens. In the latter they also observed a switching of the tetragonal axis as the applied magnetic field was rotated from [001] to [010] in the (100) plane. This phenomenon is not observed in our samples at 4.2 K. This difference in observation is ascribed to the different temperatures at which the two sets of data were taken. It should be noted that marked time lags were encountered by us while monitor-

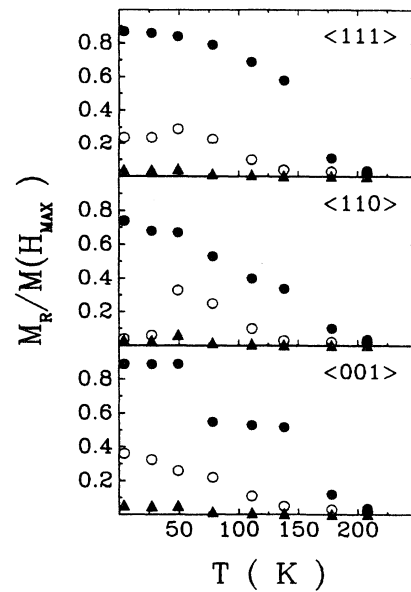


FIG. 6. Temperature variation of remanent magnetization of titanium rich specimens along the  $\langle 111 \rangle$ ,  $\langle 110 \rangle$ , and  $\langle 001 \rangle$  directions.  $\blacktriangle$ :  $x = 0.41$ ,  $\circ$ :  $x = 0.55$ ,  $\bullet$ :  $x = 0.78$ .

ing magnetization curves and hysteresis loops along all indicated directions. Below 100 K it required 1–2 min to obtain a stable reading after the magnetic field was changed. However, at 4.2 K no changes in readings were encountered in a 15-min interval. Ishikawa and Syono,<sup>7</sup> while studying the field dependence of the lattice distortion, also reported a very slow distortion of the crystals at 77 K. Thus, at 4.2 K this process is likely to be extremely slow, and the tetragonal elongation is not significantly altered by applying external field up to 15 kOe.

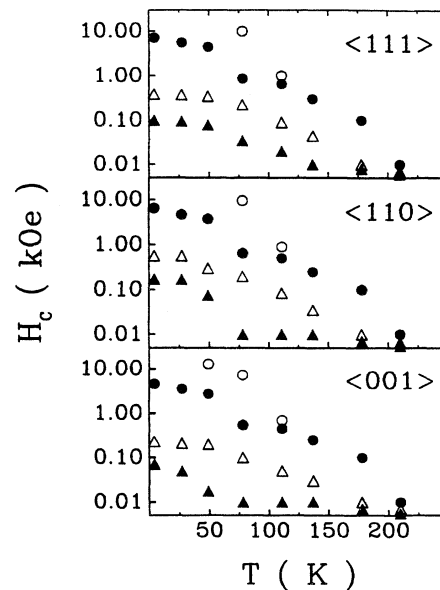


FIG. 7. Temperature variation of coercive force for Ti-rich specimens along the  $\langle 111 \rangle$ ,  $\langle 110 \rangle$ , and  $\langle 001 \rangle$  directions.  $\blacktriangle$ :  $x = 0.41$ ,  $\triangle$ :  $x = 0.55$ ,  $\bullet$ :  $x = 0.78$ ,  $\circ$ :  $x = 0.96$ .

The above is also supported by an examination of the temperature dependence of the remanent magnetization  $M_r$  and coercive force  $H_c$  along the main cubic directions, as presented in Figs. 6 and 7, respectively. The titanium-rich compounds exhibit an anomaly in the hysteresis parameters in the range 40–100 K. Below 40 K all parameters are nearly constant. These results are in good agreement with data obtained by Schmidbauer and Readman<sup>4</sup> for polycrystalline samples.

### CONCLUSIONS

We propose, on the basis of saturation-magnetization measurements, a new distribution of  $\text{Fe}^{2+}$  and  $\text{Fe}^{3+}$  ions among the tetrahedral and octahedral interstices of the  $\text{Fe}_{3-x}\text{Ti}_x\text{O}_4$  series. The calculations are based on the observation of the saturation moment and the assumed values of  $4.06 \mu_B$  and  $5 \mu_B$  for  $\text{Fe}^{2+}$  and  $\text{Fe}^{3+}$ , respectively.

It is postulated that up to the composition limit  $x=0.2$  the tetrahedral sites are occupied exclusively by  $\text{Fe}^{3+}$  ions; the conversion of  $\text{Fe}^{3+}$  into  $\text{Fe}^{2+}$  ions arising from  $\text{Ti}^{4+}$  substitution occurs solely on octahedral sites, in agreement with the Néel-Chevallier and O'Reilly-Banerjee models. At higher  $\text{Ti}^{4+}$  concentration  $\text{Fe}^{3+}$  and

for  $0 \leq x \leq 0.2$ :  $\text{Fe}^{3+}(\text{Fe}_{1-2x}^{3+}\text{Fe}_{1+x}^{2+}\text{Ti}_x^{4+})\text{O}_4$ ,

for  $0.2 < x \leq 1$ :  $\text{Fe}_{1.25-1.25x}^{3+}\text{Fe}_{1.25x-0.25}^{2+}(\text{Fe}_{0.75-0.75x}^{3+}\text{Fe}_{1.25-0.25x}^{2+}\text{Ti}_x^{4+})\text{O}_4$ .

The corresponding variations in ionic distributions, depicted in Fig. 8, are self-explanatory. The precision of the  $\text{Fe}^{2+}$ - $\text{Fe}^{3+}$  distribution among interstitial sites is limited by the accuracy of the magnetic moment measurements. Their uncertainty was estimated to be better than 0.1%, based on calibrations with Ni,  $\text{Er}_2\text{O}_3$ , and  $\text{CoHg}(\text{SCN})_4$  standards. However, for samples with  $x > 0.55$  this error is significantly larger ( $\sim 1\%$ ) because of the uncertainties in the easy axis orientation.

The variation of ionic distribution with Ti concentration shown in Fig. 8 serves as important experimental input for the subsequent analysis of various properties of titanomagnetites  $\text{Fe}_{3-x}\text{Ti}_x\text{O}_4$ ; e.g., the sharp rise of the magnetic anisotropy for  $x > 0.2$ , which will be discussed in a subsequent paper.

The angular dependence of magnetization shows that at 4.2 K the easy magnetization axis deviates from the [001] direction for specimens with  $x=0.78$  and  $x=0.96$  by about 15–25°. The plane of the deviation was not

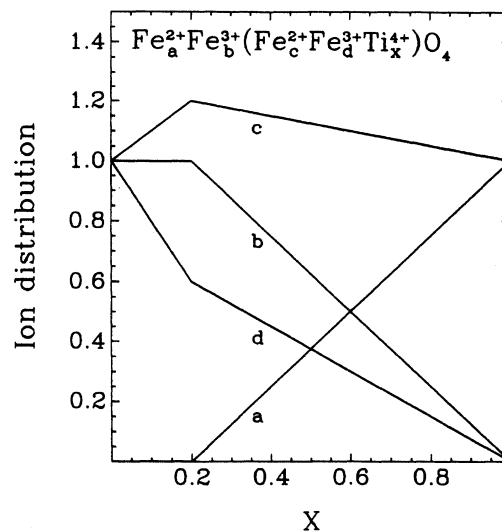


FIG. 8. Ion distribution for  $\text{Fe}_{3-x}\text{Ti}_x\text{O}_4$  series vs composition parameter  $x$ .

$\text{Fe}^{2+}$  ions are postulated to occupy both types of interstitial sublattices; their relative concentrations vary linearly with  $x$ . The two solid straight line segments in Fig. 5 correspond to the following cation distributions:

determined. Studies of low temperature hysteresis loops show anomalies of hysteresis parameters in the temperature range 40–100 K for  $x \geq 0.5$ . This is in agreement with the observation that the tetragonal distortion increases sharply in the titanium composition range  $x \geq 0.5$ <sup>5</sup> and with decreasing temperature. At 4.2 K, magnetic fields up to 15 kOe failed to switch the tetragonal distortion as well as the easy magnetization.

### ACKNOWLEDGMENTS

The authors are grateful to Professor R. Aragón, University of Delaware, for directing their attention to the problem of the ionic distribution in titanomagnetites. We are also indebted to him for the growth of some of the single crystal specimens. This research was supported by NSF Grant No. DMR 86-16533A02. J.E.S. gratefully acknowledges support from the NSF Solid-State Chemistry program DMR 89-05605.

\*Permanent address: Department of Chemistry, Ohio Northern University, Ada, Ohio 45810.

<sup>1</sup>Y. Syono and Y. Ishikawa, J. Phys. Soc. Jpn. **18**, 1230 (1963).

<sup>2</sup>Y. Syono and Y. Ishikawa, J. Phys. Soc. Jpn. **19**, 1752 (1964).

<sup>3</sup>S. K. Banerjee, W. O'Reilly, T. C. Gibb, and N. N. Greenwood, J. Phys. Chem. Solids **28**, 1323 (1967).

<sup>4</sup>E. Schmidbauer and P. W. Readman, J. Magn. Magn. Mater. **27**, 114 (1982).

- <sup>5</sup>Y. Syono, Y. Fukai, and Y. Ishikawa, *J. Phys. Soc. Jpn.* **31**, 471 (1971).
- <sup>6</sup>K. Kose, A. Ueki, and S. Iida, *J. Phys. Soc. Jpn.* **47**, 77 (1979).
- <sup>7</sup>Y. Ishikawa and Y. Syono, *J. Phys. Soc. Jpn.* **31**, 461 (1971).
- <sup>8</sup>Y. Ishikawa and Y. Syono, *Phys. Rev. Lett.* **26**, 1335 (1971).
- <sup>9</sup>Y. Ishikawa, S. Sato, and Y. Syono, *J. Phys. Soc. Jpn.* **31**, 452 (1971).
- <sup>10</sup>M. Kataoka, *J. Phys. Soc. Jpn.* **36**, 456 (1974).
- <sup>11</sup>S. Akimoto, T. Katsura, and M. J. Yoshida, *J. Geomagn. Geoelectr.* **9**, 165 (1957).
- <sup>12</sup>L. Néel, *Adv. Phys.* **4**, 191 (1955).
- <sup>13</sup>R. Chevallier, J. Bolfa, and S. Mathieu, *Bull. Soc. Fr. Mineral. Cristallogr.* **78**, 307 (1955).
- <sup>14</sup>W. O'Reilly and S. K. Banerjee, *Phys. Lett.* **17**, 237 (1965).
- <sup>15</sup>A. Stephenson, *Geophys. J. R. Astron. Soc.* **18**, 199 (1969).
- <sup>16</sup>U. Bleil, *Z. Geophys.* **37**, 305 (1971).
- <sup>17</sup>U. Bleil, *Pure Appl. Geophys.* **114**, 165 (1976).
- <sup>18</sup>B. A. Wechsler, D. H. Lindsey, and C. T. Prewitt, *Am. Mineral.* **69**, 754 (1984).
- <sup>19</sup>J. B. O'Donovan and W. O'Reilly, *Phys. Chem. Minerals* **5**, 255 (1979).
- <sup>20</sup>H. R. Harrison and R. Aragón, *Mater. Res. Bull.* **13**, 1097 (1978).
- <sup>21</sup>R. Aragón, D. J. Buttrey, J. P. Shepherd, and J. M. Honig, *Phys. Rev. B* **31**, 430 (1985).
- <sup>22</sup>J. P. Shepherd and C. J. Sandberg, *Rev. Sci. Instrum.* **55**, 1696 (1984).
- <sup>23</sup>R. Aragón and R. H. McCallister, *Phys. Chem. Minerals* **8**, 112 (1982).
- <sup>24</sup>J. M. Honig and R. Aragón, *Z. Anorg. Allg. Chem.* **540/541**, 80 (1986).
- <sup>25</sup>S. Akimoto, *J. Phys. Soc. Jpn.* **17** (SB1), 706 (1961).
- <sup>26</sup>G. Blasse, *Philips Res. Rep. Suppl. No. 3* (1964).
- <sup>27</sup>E. J. W. Verwey and E. L. Heilmann, *J. Chem. Phys.* **15**, 174 (1947).